Controlling and Maximizing the Humanoid Robot Pushing Force by Postures

Youngbum Jun, Alex Alspach and Paul Oh
Drexel University
Department of Mechanical Engineering and Mechanics
3141 Chestnut Street
Philadelphia, PA 19104
youngbum.jun@drexel.edu, alex.alspach@drexel.edu, and paul@coe.drexel.edu

***Abstract*—Pushing is one of the strategies in the object manipulation that requires to interact with environment. Many force control approaches have been proposed for such manipulation. In a force controller impementation for a humanoid robot, however, it must be considered that the humanoid robot does not have a fixed point to the ground. If the reaction force is greater than the ability that a humanoid robot can support, the robot will lose its balance. This paper represents a method to increase and decrease the force limitation of a humanoid robot by changing its posture. Based on Double Inverted Pendulum (DIP) model, the force limitation that the humanoid robot can support is calculated. With feet-apart strategy and whole-body posture, the author proposes how to maximize the force limitation in a certain condition where the height of the target object is set. Through comparision the simulation with experimental data, the analysis and approaches described in this paper are evaluated and validated.**

***Index Terms*—Hubo, Whole-body Posture, Pushing, Force limitation**

I. Introduction

No matter what types of the target object, the horizontal and vertical force is only force that results a translational motion of the object in three dimensional dynamics. It is a part of Newton's law. In a point of view of human daily life, such relationship can be easily understood in many physical manipulation tasks. Human must generate some sort of force in order to handle an object. Human has a strategy to reproduce such force in the horizontal and vertical direction called as pushing/pulling and lifting, respectively. These are the most fundamental motion in manipulation that a humanoid robot should be able to mimic.

In terms of pushing, it is generally used to move an object in a horizontal plane. In particular, when moving an object too large or heavy to lift, a human often takes this strategy. Beyond moving an object, pushing is required to manipulate a lot of mechanisms such as doors, wheelchairs, and dollies. A pushing force may be applied when using tools like drills or wrenched or even to support an unstable object.

Pushing is an act of a physical interaction that fundamentally follows Newton's third law, action-reaction law. Many researchers in biomechanics have investigated the factors that influence the magnitude of pushing force based on measurement of its reaction force. They concluded that the pushing force is mainly determined by a posture and its maximum force is limited by the ability to displace the Center of Mass (CoM) from Center of Pressure (CoP) located on the support foot [1]. Based on such ideas, Harada et. al combined it with Zero-Moment Point (ZMP) stability criterion for the humanoid pushing [2].

The main interest in Harada's papers was the humanoid pushing in walking. To achieve such goal, they modeled a full-sized humanoid robot as Linearized Inverted Pendulum (LIPM) widely used for the humanoid walking model. To control the pushing force, they moved the position of CoM in forward and backward based on the force data on wrist. The impedance control on arms prevented a humanoid robot from losing a balance by a sort of reaction force greater than the desired pushing force. This methodology has been extended in past a decade and resulted in a full-sized humanoid robot pushing a person on wheelchair [3].

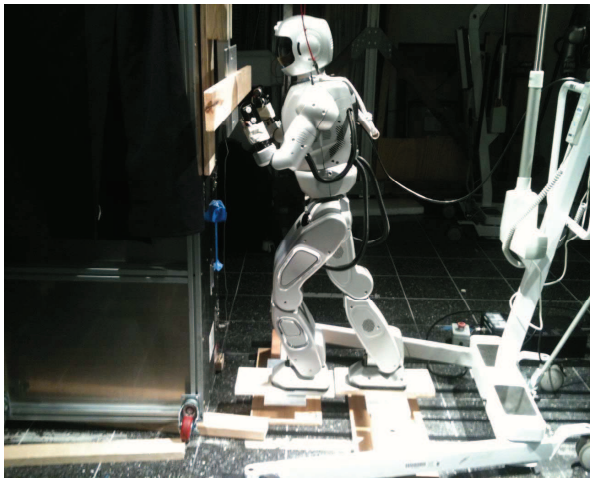

Fig. 1. Hubo+ (KHR) pushing a wall with the maximum posture in place

The previous works related to a pushing task have mainly focused on pushing in walking. The author in this paper extends such works to dynamic pushing in place. Drilling a hole is a typical example. In such applications, a humanoid robot has to interact in place with the environment directly or via a tool. In this case, the pushing force must be delicately

controlled not to break an object or tool and not to damage the humanoid robot. Many force control methods have been proposed [4] [5] and they are appropriate not to happen such situations. However, without consideration of the force limitation, the large force generated by the actuators or from the environment will result that the humanoid robot falls down since the humanoid robot is quite rigid and is not fixed to the ground. Thus, it is important to understand the force limitation that the humanoid robot can support and how to maximize and control it.

The author in this paper analyzes the relationship between the pushing force and postures and proposes a method to maximize the pushing force. With the feet-apart strategy [1] and utilizing the upper body, the force-posture relationship is mathematically derived and the maximum pushing posture is introduced. Through the actual experiments with a full-sized humanoid robot named as Hubo [6], author's approach is evaluated and validated.

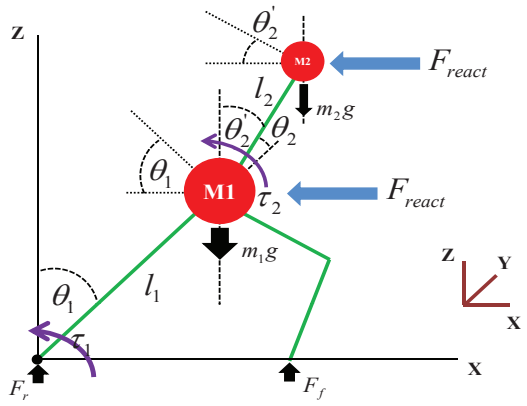

Fig. 2. A force model of Double Inverted Pendulum in a static posture

II. Dynamic Model with External Force

Harada et. al [2] derived the linear relationship between the Zero-Moment Point (ZMP) and reaction force based on cart-table inverted pendulum model [8]. The author extends such relationship into that with DIP model.

A. Double Inverted Pendulum Model

The Doulbe Inverted Pendulum (DIP) [7] is one of the dynamic models to utilize the upper body. Figure.2 represents a 2-dimentional kinematics and dynamics of DIP with the feet-apart posture. The origin in Figure.2 stands for the ankle joint in the rear leg. m_1 and m_2 are lower body point mass and upper body point mass, respectively. In this paper, the author assumes that m_1 and m_2 are located in the hip and chest, respectively, and the lower body link, l_1, and upper body link, l_2, are rotating with respect to the ankle and hip joints, respectively, in the humanoid robot. τ_1 and τ_2 denote the torque acting on the ankle joint of the rear leg and the hip joint. The dynamic equation of DIP without the external force is (1).

$$\begin{bmatrix}\tau_1\\ \tau_2\end{bmatrix} = M(\theta)\ddot{\theta} + V(\theta,\dot{\theta}) + G(\theta) \tag{1}$$

Where M is 2×2 inertial matrix, V is 2×2 centrifugal and coriolis part, and G is 2×2 gravitional constant.

Note that the author ignores the torque acting on the ankle joint of the front foot since the location of the front foot will be determined by []. It means that the role of that torque for ZMP is very small when the external force is applied. Also note that the mass of the front leg is ignored but should be considered. This modeling error is shown in the experimental results.

B. Relationship between Zero-Moment Point and External Force

In the static posture, the acceleration and velocity of upper limb and lower limb can be ignored. Accordingly, (1) remains only gravitional part and is shown as (2).

$$\begin{bmatrix}\tau_1\\ \tau_2\end{bmatrix} = \begin{bmatrix}-(m_1+m_2)l_1 g\sin(\theta_1) - m_2 l_2 g\sin(\theta_1+\theta_2)\\ -m_2 l_2 g\sin(\theta_1+\theta_2)\end{bmatrix} \tag{2}$$

In this case, the ZMP equation is simply defined as (3). Thus, the ZMP in the forward direction, X, is as shown as (4).

$$\frac{-\tau_1}{F_z} = ZMP = \frac{-\tau_1}{(m_1+m_2)g} \tag{3}$$

$$ZMP_x = l_1\sin(\theta_1) + \frac{m_2}{m_1+m_2} l_2\sin(\theta_1+\theta_2) \tag{4}$$

Where F_z is the ground reaction force that equals to $(m_1+m_2)g$.

With the external force, τ_1 which is the joint torque on the ankle of the rear leg is defined as (5).

$$\tau_1 = -(m_1+m_2)l_1 g\sin(\theta_1) - m_2 l_2 g\sin(\theta_1+\theta_2) + \tau_{react} \tag{5}$$

$$\tau_{react} = F_{react}(l_1\cos(\theta_1) + l_2\cos(\theta_1+\theta_2)) \tag{6}$$

With (3), the important relationship between the horizontal reaction force in a given posture is derived in (7).

$$\frac{1}{a}\triangle ZMP = \triangle F_{react} \tag{7}$$

$$\text{Where } a = \frac{l_1\cos(\theta_1) + l_2\cos(\theta_1+\theta_2)}{(m_1+m_2)g}$$

Since $\theta_1 + \theta_2$ are numeric values that can be obtained from a given posture. Thus, the relationship between the reaction force and ZMP is linear. It is the same result as in [2].

III. Feet-apart Strategy and Maximum Pushing Posture

The feet-apart strategy [1] is a posture with a stretched rear leg. Human naturally uses this strategy in many pushing tasks in order to maximize the pushing force. Also, human changes the lower and upper body posture simultaneously to handle the magnitude of the maximum pushing force.

A. Feet-apart Posture on Humanoid Robot

The foot location of the rear leg can be easily calculated from the location of m_1. Now, the foot location of the front leg has to be determined. The front leg does not affect the magnitude of the pushing force dominantly but play an important role in stability and manipulability of a humanoid robot while pushing. (8) is the boundary condition of minimum displacement of the front foot.

$$d \geqq \frac{(m_1+m_2)l_1 g\sin(\theta_1) + m_2 l_2 g \sin(\theta_1+\theta_2)}{(m_1+m_2)g} \tag{8}$$

Where d is the displacement from the rear foot location.

It is obvious that if the initial ZMP without the reaction force is further than the front foot, the humanoid robot will fall down to the forward direction. On the other hands, if the front leg is stretched toward the forward direction, the support polygon becomes the largest but manipulability is the smallest since the lower body cannot move. Thus the front foot location should be determined based on the specific pushing task.

Note that it is important to align the rear foot and ZMP locations with the line of the force direction. If not, the humanoid robot will lose its balance.

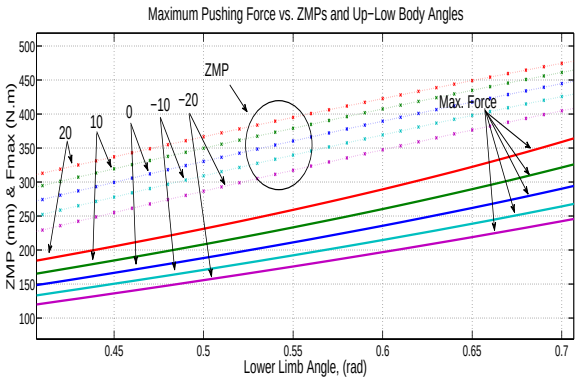

Fig. 3. Maximum pushing force vs. ZMPs and Postures

B. Force Limitation

Based on (7), the ZMP is moving from the initially placed position to the rear support foot when pushing force is applying to the target obejct. Assume that friction is enough for the humanoid robot to tip over, the humanoid robot starts to tip while the ZMP is passing through the location of the rear foot. Mathematically such condition can be defined as $\tau_1 = 0$. Thus the pushing force of a given posture can be calculated using (3) and (9).

$$F_{max} = \frac{(m_1+m_2)l_1 g\sin(\theta_1) + m_2 l_2 g \sin(\theta_1+\theta_2)}{l_1\cos(\theta_1) + l_2\cos(\theta_1+\theta_2)} \tag{9}$$

Where F_{max} is the force limitation that the humanoid robot can support. As long as there is no vertical force pressing the humanoid robot down, (9) is valid. Thus, the force controller to manipulate the target object should be designed within the force limitation and its performance should not exceeds that force so as to keep the balance while carrying out a pushing task.

C. Posture for Maximum Pushing Force

In previous works [1][2][3], they controls the pushing force by horizontally changing the position of CoM while the upper body is upright to the ground in order to keep the height of the contact point between the arms and object. With this idea, the author controls the pushing force using both lower and upper body simultaneously while maintaining the height of the contact point.

Assume that the humanoid robot initially poses and the height of the target object is specified as in (10).

$$P_h = l_1\sin(\theta_1) + l_2\sin(\theta_1+\theta_2) = const. \tag{10}$$

Where P_h is the pushing height. All possible postures with the constant hieght will satisfy the condition shown in (11).

$$P_h = l_1\sin(\theta_1') + l_2\sin(\theta_1'+\theta_2') \tag{11}$$

Where θ_1' and θ_2' are the angle of the lower body and upper body, respectively. Using (11), the posture that has maximum pushing force in a given initial posture and height of the object can be obtained by (12).

$$max[\theta_1,\theta_2] = max\left(\frac{(m_1+m_2)l_1 g\sin(\theta_1') + m_2 l_2 g\sin(\theta_1'+\theta_2')}{l_1\cos(\theta_1') + l_2\cos(\theta_1'+\theta_2')}\right) \tag{12}$$

IV. Simulation and Experiment

The Hubo+ developed by KAIST in South Korea is used for simulation and experiments. The max. length from hip and ankle joint is 560mm, and the length of hip joint to chest is 367mm. Also the distance between center of the robot to hip joint in lateral direction is 88.5mm. The total weight is 47kg. Based on such parameters, the author set the lower body mass and upper body mass as 30kg and 17kg, respectively.

A. Simulation

Figure.3 represents the simulation data of (9). There are five dotted lines for ZMPs and five bold lines for force limitation (Max. Force) that correspond to the ZMP lines. The line at the top in the dotted group is the ZMP plot based on the lower body angle that varies from 0.45 to 0.7 rad and upper body angle that equals to 20deg. The force plot corresponding to that ZMP plot is shown at the top in the bold group. With the same manner, each dotted line for ZMP from the bottom to the top shows the upper limb angle from -20, -10, 0, 10, and 20deg and corresponds to each bold line for force limitation from the bottom to the top, respectively.

There are two facts that must be emphasized. First, the force limitation of each posture is unique. Secondly, even if some postures have the same ZMP values, the force limitations are different from each other because of the different upper body angles. It gives an idea that there is an unique posture that can produce the maximum pushing force in accordance with the height of the contact point.

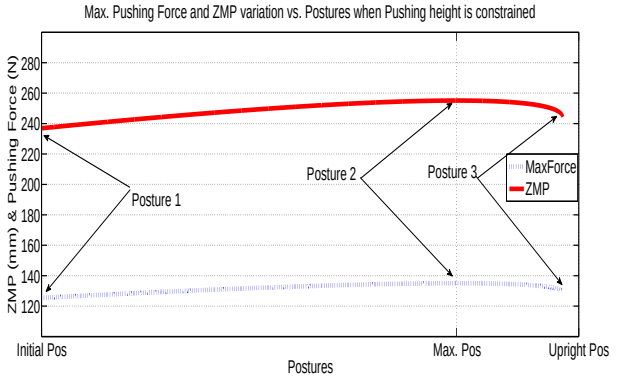

Fig. 4. Maximum pushing force and ZMP variation from posture 1 to posture 3

In Figure. 4 shows the pushing force and ZMP variation with the different posture when the contact point is specified. To clarify, the arrow named Posture 1 in Figure. 4 indicates the maximum pushing force (red and bold line) and ZMP (blue and dot line) of the robot posing (a) in Figure. 5. The arrow named Posure 2, and Posture 3 also point both maximum pushing force and ZMP, and corresponds to (b) and (c) in Figure. 5, respectively. (a) in Figure. 5 is the initial posture. (b) and (c) are the posture of the maximum pushing force and the upright posture obtained from (12), respectively. Posture 1, (a) in Figure.5, is the initial posture when $\theta_1 = 20\,\text{deg}$ and $\theta_2 = 0\,\text{deg}$. Posture 2, (b), shows the maximum pushing force posture when $\theta_1 = 24.63\,\text{deg}$ and $\theta_2 = -15.21\,\text{deg}$ and (c) is the upper body upright posture when $\theta_1 = 25.81\,\text{deg}$ and $\theta_2 = -25.60\,\text{deg}$.

In the simulation result in Figure. 4, there is an unique posture that can generate the maximum pushing force without changing the height of the contact point. Beyond our simulation, the humanoid robot can achieve the maximum pushing posture using lower and upper body angles.

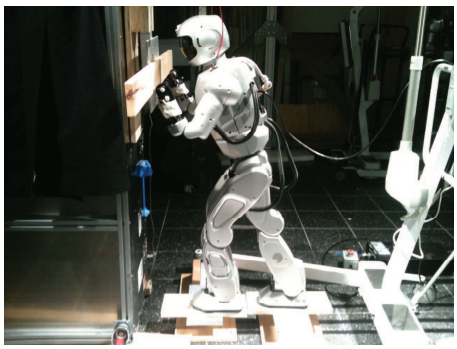

(a)

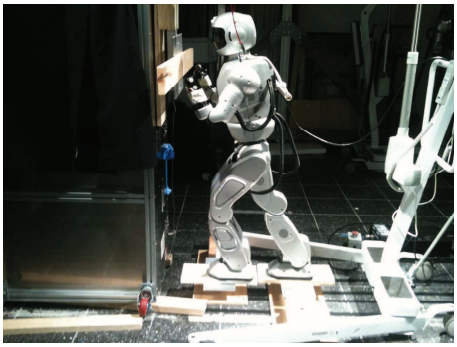

(b)

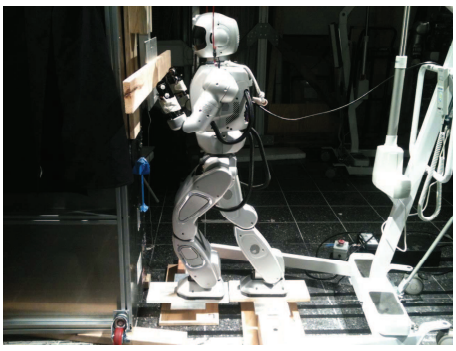

(c)

Fig. 5. Experiments. (a) Initial posture, (b) Maximum pushing posture, and (c) Upperbody upright posture.

B. Hubo+ Experimental Result

Figure. 5 shows the experimental set up. The reaction force and ground reaction force on each foot are recorded while

hubo+ is pushing the wall. Figure. 6 represents the reaction force vs. ZMP plot of posture 1, 2, and 3. The experimental data in Figure. 6 is exactly same as what we expected in Figure. 4.

Figure. 7 describes the comparison between the simulation data in Figure. 4 and the experimental data. (a), (b), and (c) in Figure. 7 denotes posture 1, 2, and 3, respectively. The blue and bold line in each plot stands for the simulation data using DIP model and the read and dot line in each graph means the experimental data from Hubo+.

There are two significant error presented in Figure. 7. The first error is the magnitude of the force limitation and the second is the slope. Both are caused by modeling uncertainty and robot's stiffness. Such error should be minimized so as to set the proper force limitation. Using system identification method, the parameters in DIP model will be estimated in the future work.

V. Conclusion

The author in this paper explained the force limitation in terms of the humanoid posture and proposed a method to maximize the pushing force. The idea was inspired by the human pushing motion. To maximize the pushing force, the author employed the feet-apart strategy to strech the support leg in a static posture and controlled the lower and upper angles to obtain the posture that can produce the maximum pushing force. Double Inverted Pendulum (DIP) model was used as a dynamic model of the humanoid robot. Based on such model, the author demonstrated the relationship between the force limitation and Zero-Moment Point according to the posture. Through the actual implementation on Hubo+, the proposed force analysis and postures are evaluated. But there was still modeling uncertainty. It resulted in an error between the model and actual robot. It will be considered in our future works.

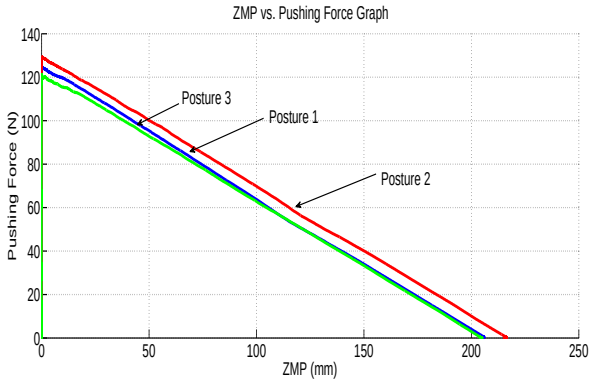

Fig. 6. ZMP vs. Pushing force

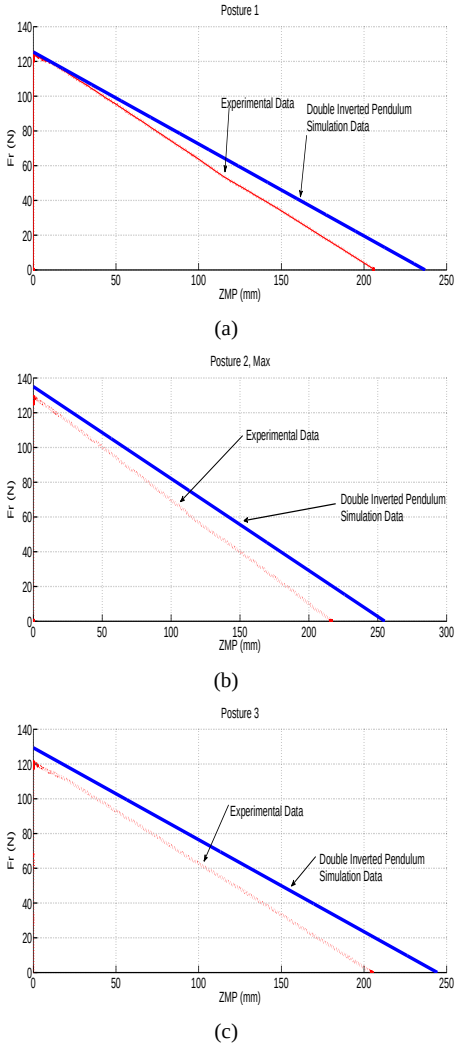

Fig. 7. ZMP vs. Pushing force. (a) Initial posture, (b) Maximum pushing posture, and (c) Upperbody upright posture.

References

[1] Rancourt,Denis and Hogan,Neville, "Dynamics of Pushing", *Journal of motor behavior*, V33, N4, pp.351-362, 2001

[2] Harada, K.; Kaneko, M., "Whole body manipulation", *Intelligent Syst. Inst., Nat. Inst. of Adv. Ind. Sci. and Technol.*, V1, pp.190-195, 2003, Tsukuba, Japan

[3] Nozawa, S., Kakiuchi, Y., Okada, K., Inaba, M. "Controlling the planar motion of a heavy object by pushing with a humanoid robot using dual-arm force control", *Robotics and Automation, ICRA, IEEE Int. Conf. on*,pp.1428-1435, 2004, Saint Paul, MN, USA

[4] Hogan, N., "Impedance Control: An Approach to Manipulation: Part I - Theory", pp. 1-7, "Part II -Implementation", pp. 8-16, "Part 111 - Applications", pp. 17-24, *ASME Journal of Dynamic Systems, Measurement and Control*, Nov. 107, 1985

[5] Whitney, D. (1977) "Force Feedback Control of Manipulator Fine Motions", *Journal of Dynamic Systems, Measurement and Control*, pp. 91-97

[6] Kim, J.H., Oh, J.H.,"Walking Control of the Humanoid Platform KHR-1 based on Torque Feedback Control", *IEEE International Conference on Robotics and Automation (ICRA)*, Barcelona, Spain, April 2004.

[7] Napoleon, Shigeki, N., Mitsuji, S., "Balance Control Analysis of Humanoid Robot based on ZMP Feedback Control", *Int. Conf. on Intelligent Robots and Systems*, V3, pp.2437-2442, 2002, Lausanne, Switzerland

[8] Kajita, S., Kanehiro, F., Kaneko, K., Fujiwara, K., Harada, K., Yokoi, K., Hirukawa, H., "Biped Walking Pattern Generation Using Preview Control of the Zero-Moment-Point", *IEEE Int. Conf. on Robotics and Automation (ICRA2003)*, Taipei, Taiwan, V2, pp.1620-1626, Sept. 2003